

## **CHAPTER 2**

### **Evolution of the C<sub>30</sub> Carotenoid Synthase CrtM for Function in a C<sub>40</sub> Pathway**

Material from this chapter appears in *Evolution of the C<sub>30</sub> Carotenoid Synthase CrtM for Function in a C<sub>40</sub> Pathway*, Daisuke Umeno, Alexander V. Tobias, and Frances H. Arnold, Journal of Bacteriology 184(23): 6690-6699 (2002) and is reprinted with permission from the American Society for Microbiology.

## SUMMARY

The C<sub>30</sub> carotene synthase CrtM from *Staphylococcus aureus* and the C<sub>40</sub> carotene synthase CrtB from *Erwinia uredovora* were swapped into their respective foreign C<sub>40</sub> and C<sub>30</sub> biosynthetic pathways (heterologously expressed in *Escherichia coli*) and evaluated for function. Each displayed negligible ability to synthesize the natural carotenoid product of the other. After one round of mutagenesis and screening, we isolated 116 variants of CrtM able to synthesize C<sub>40</sub> carotenoids. In contrast, we failed to find a single variant of CrtB with detectable C<sub>30</sub> activity. Subsequent analysis revealed that the best CrtM mutants performed comparably to CrtB in an *in vivo* C<sub>40</sub> pathway and that Phe 26 of CrtM is a key specificity-determining residue. The CrtM mutants showed significant variation in performance in their original C<sub>30</sub> pathway, indicating the emergence of enzymes with broadened substrate specificity as well as those with shifted specificity. We also report for the first time the isolation of carotenoid pigments based on a C<sub>35</sub> carbon backbone formed by condensation of farnesyl diphosphate (FPP) and geranylgeranyl diphosphate (GGPP) by wild-type and variants of CrtM. The expanded substrate and product range of the CrtM mutants reported herein highlights the potential for creating further new carotenoid backbone structures.

## INTRODUCTION

A common feature of small molecule natural product biosynthetic pathways is the extensive use of enzymes with broad substrate and product specificities. Many isoprenoid biosynthetic enzymes, for example, accept a variety of both natural and unnatural substrates (27, 28, 31). Some have been shown to synthesize an impressively large number of compounds (sometimes >50) from a single substrate (9, 12, 45). Natural product biosynthetic pathways also use enzymes with remarkably stringent specificity. Such enzymes are frequently seen in key determinant positions, usually in the very early steps of a pathway, while promiscuous enzymes tend to be located further downstream. Thus, many natural product pathways have a “reverse tree” topology (3, 42) where the backbone structures of metabolites are dictated by a small number of stringent, upstream enzymes. When the substrate or product preferences of these key upstream enzymes are altered, pathway branches leading to sets of novel compounds may be opened (10). Our interest is to achieve the same by applying methods of directed enzyme evolution to recombinant pathways in *Escherichia coli* (43, 50).

Among the most widespread of all small molecule natural products, carotenoids are natural pigments that play important biological roles. Some are accessory light-harvesting components of photosynthetic systems, while others are photo-protecting antioxidants or regulators of membrane fluidity. Recent studies advocate their effectiveness in preventing cancer and heart disease (26) as well as their potential hormonal activity (4, 18). Such diverse molecular functions justify exploring rare or novel carotenoid structures. At present, ~700 carotenoids from the naturally occurring C<sub>30</sub> and C<sub>40</sub> carotenoid biosynthetic pathways have been characterized (17). Most natural

carotenoid diversity arises from differences in types and levels of desaturation and other modifications of the C<sub>40</sub> backbone. C<sub>40</sub> carotenoids are also much more widespread in nature than their C<sub>30</sub> counterparts. The former are synthesized by thousands of plant and microbial species, whereas the latter are known only in a select few bacteria (46, 48). Homocarotenoids (carotenoids with >40 carbon atoms) and apocarotenoids (carotenoids with <40 carbon atoms), which result from the action of downstream enzymes on a C<sub>40</sub> substrate, are also known. Although these structures do not have 40 carbon atoms, they are nonetheless derived from C<sub>40</sub> carotenoid precursors (5).

The first committed step in carotenoid biosynthesis is the head-to-head condensation of two prenyl diphosphates catalyzed by a synthase enzyme (**Figure 2.1**). The C<sub>40</sub> carotenoid phytoene is synthesized by the condensation of two molecules of geranylgeranyl diphosphate (GGPP, C<sub>20</sub>PP) catalyzed by the synthase CrtB. (Most phytoene synthases produce the 15Z isomer of phytoene (5)). C<sub>30</sub> carotenoids are synthesized via an independent route whereby two molecules of farnesyl diphosphate (FPP, C<sub>15</sub>PP) are condensed to (15Z)-4,4'-diapophytoene by CrtM (48). The various downstream modification enzymes possess broad substrate specificity and therefore represent potential targets for generating biosynthetic routes to novel carotenoids. For example, when the three-step phytoene desaturase CrtI from *Rhodobacter sphaeroides* was replaced with a four-step enzyme from *Erwinia herbicola*, the cells accumulated a series of carotenoids produced neither by *Erwinia* nor *Rhodobacter* (16). Carotene desaturases (39), carotene cyclases (44), and  $\beta,\beta$ -carotene cleavage enzyme (40) have also been shown to accept a broad range of substrates. Combinatorial expression of such enzymes can create unusual and sometimes previously unidentified carotenoids (1, 2, 21).

Nevertheless, the greatest potential to further extend carotenoid biosynthetic diversity lies in creating whole new backbone structures, and therefore with engineering the carotene synthases.

The C<sub>30</sub> and C<sub>40</sub> pathways are very similar except in the sizes of their precursor molecules and their distributions in nature, and it is clear that they diverged from a common ancestral pathway. We would like to determine the minimal genetic change required in key carotenoid biosynthetic enzymes to create such new pathway branches. Can the enzymes that synthesize one carotenoid be modified in a laboratory evolution experiment to synthesize others? How much of carotenoid diversity can be accessed in this way? And, can *novel* pathways to different, even unnatural structures (e.g., C<sub>35</sub>, C<sub>45</sub>, C<sub>50</sub>, or larger carotenoids) be accessed by using C<sub>30</sub> or C<sub>40</sub> enzymes as a starting point? To begin to answer these questions, we studied the performance of the C<sub>30</sub> carotene synthase CrtM from *Staphylococcus aureus* in a C<sub>40</sub> pathway and the C<sub>40</sub> carotene synthase CrtB from *Erwinia uredovora* in a C<sub>30</sub> pathway. We then examined the ability of these enzymes to adapt to their respective “foreign” pathways in order to assess the ease and uncover the mechanisms by which this might be accomplished.

## RESULTS AND DISCUSSION

### Constructing pathways for C<sub>30</sub> and C<sub>40</sub> carotenoids

To establish a recombinant C<sub>40</sub> pathway in *E. coli*, we subcloned *crtE* encoding GGPP (C<sub>20</sub>PP) synthase, *crtB* encoding phytoene synthase, and *crtI* encoding phytoene desaturase, all from *E. uredovora*, into a vector derived from pUC18, resulting in plasmid pUC-*crtE-crtB-crtI* (**Figure 2.2a**). For C<sub>30</sub> carotenoid production, plasmid pUC-*fps-crtM-*

*crtN* was constructed by integrating the *E. coli* farnesyl diphosphate (C<sub>15</sub>PP) synthase (FPS) gene, *fps*, with *crtM* (4,4'-diapophytoene synthase gene) and *crtN* (4,4'-diapophytoene desaturase gene) from *S. aureus* into the same vector. Plasmid pUC-*crtM-crtN* was constructed in an identical fashion, but it lacks *fps*. Each plasmid shares the cloning sites for the corresponding enzyme genes: *Eco*RI and *Xba*I sites flank isoprenyl diphosphate synthase (IDS) genes (*crtE* and *fps*), *Xba*I and *Xho*I sites flank carotene synthase genes (*crtB* and *crtM*), and *Xho*I and *Apa*I sites flank carotene desaturase genes (*crtI* and *crtN*) (**Figure 2.2a**). With this arrangement, corresponding genes could be easily swapped in order to evaluate their function in the other pathway.

*E. coli* cells harboring pUC-*crtE-crtB-crtI* plasmids (C<sub>40</sub> pathway) developed a characteristic red-pink color, whereas cells possessing pUC-*fps-crtM-crtN* and pUC-*crtM-crtN* plasmids (C<sub>30</sub> pathway) were yellow (**Figure 2.2b**). HPLC analysis of extracted pigments showed that XL1-Blue(pUC-*crtE-crtB-crtI*) cells produce mostly lycopene (four-step desaturation) along with a small amount (5 to 10% of total pigment) of 3,4,3',4'-tetrahydrolycopene (six-step desaturation) under the conditions described. Although CrtI is classified as a four-step desaturase, production of 3,4-didehydrolycopene (five-step desaturation) by CrtI both *in vivo* and *in vitro* has been reported (15, 23).

Several groups have expressed CrtM and CrtN from *S. aureus* in *E. coli* and observed almost exclusive production of 4,4'-diaponeurosporene (39, 51). However, in our XL1-Blue(pUC-*crtM-crtN*) expression system, the cells accumulated a significant amount of 4,4'-diapolycopene (~30% of total carotenoids). When a constitutive *lac* promoter (lacking the operator) was used for operon expression, the amount of 4,4'-

diapolycopene increased further and reached 50% of carotenoids produced (D. Umeno, unpublished data). This phenomenon was observed in all *E. coli* strains we tested, BL21, BL21(DE3), JM109, JM101, DH5 $\alpha$ , HB101, SCS110, and XL10-Gold, and was insensitive to growth temperature and plasmid copy number. Thus, it is clear that the apparent desaturation step number of CrtN depends on its expression level and the effective concentration of substrates.

In *E. coli*, FPP (C<sub>15</sub>PP) is a precursor to a variety of important housekeeping molecules such as respiratory quinones, prenylated tRNA, and dolichol. Concerned about retarding or preventing the growth of our recombinant C<sub>30</sub> cultures due to depletion of FPP, we first expressed the *fps* gene along with *crtM* and *crtN*. However, we observed no difference in growth rate, pigmentation level, or carotenoid composition between XL1-Blue cells harboring the pUC-*crtM-crtN* plasmid and those harboring the pUC-*fps-crtM-crtN* plasmid. This demonstrates that endogenous FPP levels in *E. coli* suffice to support both growth and synthesis of C<sub>30</sub> carotenoids.

### **Functional analysis of CrtM and CrtB swapped into their respective foreign pathways**

To assess the function of wild-type CrtM in a C<sub>40</sub> pathway, pUC-*crtE-crtM-crtI* was constructed and transformed into *E. coli* XL1-Blue. Under these circumstances, CrtM is supplied with GGPP (C<sub>20</sub>PP) produced by CrtE. If CrtM were able to synthesize the C<sub>40</sub> carotenoid phytoene from GGPP, subsequent desaturation by CrtI to lycopene would cause the cells to develop a red-pink color. However, while cells expressing the *crtE-crtB-crtI* operon exhibited the characteristic red-pink of lycopene (**Figure 2.2b**) and synthesized this carotenoid in liquid culture (**Figure 2.4**), cells expressing the *crtE-crtM-*

*crtI* operon had only very subtle pink-orange color on agar plates and synthesized much less lycopene in liquid culture (**Figure 2.4**). As did Raisig and Sandmann (39), we thus conclude that CrtM fails to complement CrtB in a C<sub>40</sub> pathway and has very poor ability compared to CrtB to synthesize the C<sub>40</sub> carotenoid backbone. This observation cannot be explained by simple competition between FPP and GGPP for access to CrtM (coupled with poor ability of CrtI to desaturate the C<sub>30</sub> product) because XL1-Blue cells expressing the *crtE-crtM-crtN* operon showed only very minor yellow color development. This indicates that the availability of FPP for carotenoid biosynthesis is significantly reduced upon expression of CrtE.

The function of CrtB in a C<sub>30</sub> pathway was examined by analyzing the pigmentation of XL1-Blue cells transformed with pUC-*crtB-crtN*. In this case, endogenous FPP is the only available prenyl diphosphate substrate for CrtB, since the level of GGPP is very low in *E. coli* compared with that of FPP. If CrtB could synthesize C<sub>30</sub> carotenoids from FPP, the 4,4'-diapophytoene produced would be desaturated by CrtN and the cells would develop a yellow color. In contrast to the intense yellow of XL1-Blue transformed with pUC-*crtM-crtN*, XL1-Blue(pUC-*crtB-crtN*) showed no color development (**Figure 2.2b**). When expressed alone or with CrtN, CrtB synthesized C<sub>30</sub> carotenoids very poorly in liquid culture (see **Figures 2.5 and 2.6**). We thus conclude that CrtB fails to complement CrtM in a C<sub>30</sub> pathway.

We also analyzed the pigment produced by XL1-Blue carrying pUC-*fps-crtB-crtN*. In this case, the cells displayed a yellow color similar to that of XL1-Blue transformed with pUC-*fps-crtM-crtN* (**Figure 2.2b**). HPLC analysis of carotenoid extracts from XL1-Blue(pUC-*fps-crtB-crtN*) revealed the C<sub>40</sub> carotenoid neurosporene,



with trace amounts of the C<sub>30</sub> carotenoids 4,4'-diapolycopene and 4,4'-diaponeurosporene. Thus, CrtB seems to have at least some C<sub>30</sub> activity in the presence of high levels of FPP. Production of the C<sub>40</sub> carotenoid neurosporene as the major pigment is explained by the promiscuous nature of both FPS and CrtN. This was verified by our observation that cells expressing an *fps-crtB-crtI* operon had a weak pink hue and accumulated lycopene and 3,4,3',4'-tetrahydrolycopene. Thus, FPS can produce significant amounts of GGPP in *E. coli* when overexpressed. It is known that avian FPS also possesses weak ability to synthesize GGPP (41). Indeed, other studies have shown a varied product distribution and strong dependence on conditions for FPS enzymes (25, 34). Additionally, CrtN can accept phytoene as a substrate and introduce two or three double bonds (39). When we transformed XL1-Blue with pUC-*crtE-crtB-crtN*, the resulting cells exhibited significant yellow color (**Figure 2.2b**) and accumulated neurosporene, thus demonstrating the promiscuity of CrtN.

### Screening for synthase function in a foreign pathway

In the previous section, we confirmed that the carotene synthases CrtB and CrtM show negligible activity in their respective foreign pathways. We next proceeded to evolve the two enzymes, with the goal of improving the function of each in the other's native pathway. To uncover CrtB variants with significant CrtM-like ability to synthesize C<sub>30</sub> carotenoids, we constructed pUC-*[crtB]-crtN* libraries and transformed them into XL1-Blue cells. Here GGPP is not available, so cells with the wild-type *crtB-crtN* operon fail to develop color. Any variants of CrtB able to convert FPP (C<sub>15</sub>PP) into 4,4'-diapophytoene would produce yellow colonies. Similarly, we searched for CrtM mutants with improved C<sub>40</sub> activity by transforming four pUC-*crtE-[crtM]-crtI* libraries into XL1-

Blue. As described in the previous section, the amount of FPP available for carotenoid biosynthesis becomes significantly depleted when CrtE is overexpressed, resulting in negligible production of C<sub>30</sub> carotenoids, even by native C<sub>30</sub> enzymes. Cells expressing wild-type CrtM from the *crtE-crtM-crtI* operon showed a weak pink-orange color due to trace production of lycopene as well as C<sub>30</sub> and C<sub>35</sub> carotenoids, but CrtM mutants able to complement CrtB via acquisition of enhanced C<sub>40</sub> activity would be expected to yield intensely red-pink colonies and thus be distinguishable on the plates.

### **Evolution of 4,4'-diapophytoene synthase (CrtM) for function in a C<sub>40</sub> pathway**

Four different mutagenic libraries of *crtM* corresponding to four different mutation rates were generated by performing error-prone PCR (54) on the entire 843-nucleotide *crtM* gene. PCR products from each reaction were ligated into the *XbaI-XhoI* site of pUC-*crtE-crtM-crtI* (**Figure 2.2a**), resulting in pUC-*crtE-[crtM]-crtI* libraries. **Figure 2.3** shows a typical agar plate covered with a nitrocellulose membrane upon which lie colonies of *E. coli* XL1-Blue expressing a *crtE-[crtM]-crtI* library. In each library, colonies with pale orange, pale yellow, or virtually no color dominated the population. The pale orange colonies express variants of CrtM with phenotypes similar to that of the wild-type enzyme in this context, while the pale and colorless colonies express severely or completely inactivated synthase mutants. More rare were colonies that developed an intense red-pink color, indicating significant production of C<sub>40</sub> carotenoids and hence improved CrtB-like activity of CrtM. On average, about 0.5% of the colonies screened showed intense red-pink color. The highest frequency of positives was obtained from the library prepared by PCR with the lowest MnCl<sub>2</sub> concentration (0.02 mM). In this library, approximately 1 out of every 120 colonies was red-pink (0.8%). We screened

over 23,000 CrtM mutants from the four libraries and picked 116 positive clones. These clones were re-screened by stamping them onto an agar plate covered with a white nitrocellulose membrane. All 116 stamped clones exhibited red-pink coloration. We sequenced the 10 most intensely red stamped clones, as determined by visual assessment. Mutations found in these variants (**Table 2.1**) were heavily biased toward transitions: 36 versus only 3 transversions. Additionally, 87% of the base substitutions found by sequencing were A/T→G/C. This is a typical observation for PCR mutagenesis with MnCl<sub>2</sub> (7, 24). Out of 39 total nucleotide substitutions, 24 resulted in amino acid substitutions. Most notably, 9 of the 10 sequenced CrtM mutants had a mutation at phenylalanine 26.

### **Carotenoid production of evolved CrtM variants**

We analyzed in detail the *in vivo* carotenoid production of variant M<sub>8</sub>, which has the F26L mutation only; variant M<sub>9</sub>, which has the F26S mutation; and variant M<sub>10</sub>, which has no mutation at F26. To confirm the newly acquired CrtB-like function of these three sequenced variants of CrtM, XL1-Blue cultures carrying each of the three plasmids pUC-*crtE-M<sub>8</sub>-crtI*, pUC-*crtE-M<sub>9</sub>-crtI*, and pUC-*crtE-M<sub>10</sub>-crtI* (collectively referred to as pUC-*crtE-M<sub>8-10</sub>-crtI*) were cultivated in TB medium. Extracted pigments were analyzed by HPLC with a photodiode array detector (**Figure 2.4**). These analyses revealed that all three clones produced the C<sub>40</sub> carotenoids lycopene (peak 5) and 3,4,3',4'-tetrahydrolycopene (peak 4) as major products, whereas cells harboring the parent pUC-*crtE-crtM-crtI* plasmid produced mainly C<sub>30</sub> and trace amounts of C<sub>40</sub> and C<sub>35</sub> carotenoids. Two carotenoids with C<sub>35</sub> backbone structures were detected in extracts from cells harboring pUC-*crtE-crtM-crtI* and pUC-*crtE-M<sub>8-10</sub>-crtI*. Elution profiles, UV-visible

spectra, and mass spectra confirm that one of the structures is the fully conjugated C<sub>35</sub> carotenoid 4-apo-3',4'-didehydrolycopene. We also detected C<sub>35</sub> carotenoids with 11 conjugated double bonds. Because C<sub>35</sub> carotenoids are asymmetric, there are two possible C<sub>35</sub> structures that possess 11 conjugated double bonds: 4-apolycopene and 4-apo-3',4'-didehydro-7,8-dihydrolycopene. At present, we have not determined whether the cells synthesize one (and if so, which one) or both of these C<sub>35</sub> carotenoids.

### **Direct product distribution of CrtM variants in the presence of GGPP (C<sub>20</sub>PP)**

To directly evaluate the product specificities of the three CrtM mutants, we constructed pUC-*crtE-M<sub>8-10</sub>* plasmids and transformed the plasmids into XL1-Blue cells. Here the CrtM variants are supplied with GGPP, but the carotenoid products cannot be desaturated. Because all three possible products in this scenario, 4,4'-diapophytoene (C<sub>30</sub>), 4-apophytoene (C<sub>35</sub>), and phytoene (C<sub>40</sub>), have an identical chromophore structure consisting of three conjugated double bonds, the molecular extinction coefficients for all three can be assumed to be equivalent, irrespective of the total number of carbon atoms in the carotenoid molecule (49). Thus, the product distribution of the CrtM variants can be discerned from the HPLC chromatogram peak heights (at 286 nm) for each product. As can be seen in **Figure 2.5**, cultures expressing CrtB along with CrtE produced approximately 230 nmol of phytoene/g of dry cell mass but did not detectably synthesize C<sub>30</sub> or C<sub>35</sub> carotenoids. CrtE-CrtM cultures produced about 20 to 35 nmol of each of the C<sub>30</sub>, C<sub>35</sub>, and C<sub>40</sub> carotenoids/g. In stark contrast, CrtE-M<sub>8</sub> and CrtE-M<sub>9</sub> cultures, which express synthases mutated at F26, generated over 300 nmol of phytoene/g. These cultures also produced 40 to 75% more C<sub>35</sub> carotenoids but 70 to 90% fewer C<sub>30</sub> carotenoids than CrtE-CrtM cultures. Cultures expressing M<sub>10</sub>, which has no mutation at F26, along with

CrtE synthesized roughly 100 nmol of phytoene/g as well as about 20 and 14 nmol of C<sub>35</sub> and C<sub>30</sub> carotenoids/g, respectively.

### **Comparison of the C<sub>40</sub> and C<sub>30</sub> performance of CrtM variants**

To compare the acquired CrtB-like C<sub>40</sub> function of the CrtM mutants with their CrtM-like ability to synthesize C<sub>30</sub> carotenoids, the three mutants were placed back into the original C<sub>30</sub> pathway, resulting in pUC-*M*<sub>8-10</sub>-*crtN* plasmids. Pigmentation analysis of cells carrying these as well as pUC-*crtE-M*<sub>8-10</sub>-*crtI* plasmids (**Figure 2.6**) revealed that the CrtM variants retained C<sub>30</sub> activity, although the C<sub>30</sub> pathway performance of cells expressing these mutants varied. Acetone extracts of cultures expressing variant M<sub>8</sub>, which has the F26L mutation alone, along with CrtE and CrtI (CrtE-M<sub>8</sub>-CrtI cultures) had more than threefold-higher C<sub>40</sub> carotenoid absorbance (475 nm) than extracts of CrtE-CrtM-CrtI cultures. However, the C<sub>30</sub> carotenoid absorbance (470 nm) of extracts of cultures expressing variant M<sub>8</sub> and CrtN was only about 40% that of CrtM-CrtN cultures. Cultures expressing variant M<sub>9</sub>, which has the F26S mutation, along with CrtE and CrtI also yielded extracts with over three times the C<sub>40</sub> signal of CrtE-CrtM-CrtI culture extracts. Yet the C<sub>30</sub> signal of M<sub>9</sub>-CrtN culture extracts was only about 10% that of CrtM-CrtN culture extracts. Cultures expressing mutant M<sub>10</sub>, which has no mutation at F26, along with CrtE and CrtI generated extracts with approximately 70% higher C<sub>40</sub> absorbance than extracts of CrtE-CrtM-CrtI cultures. Interestingly, cultures expressing M<sub>10</sub> and CrtN showed no reduction in C<sub>30</sub> pathway performance compared to CrtM-CrtN cultures. M<sub>10</sub> was the only one of the 10 sequenced variants that gave this result (data not shown).

### Analysis of mutations

The most significant and only recurring mutations found in the 10 sequenced CrtM variants were those at F26. In seven variants, phenylalanine is replaced by leucine, while two have serine at this position. The F26L substitution alone is sufficient for acquisition of C<sub>40</sub> activity by CrtM (M<sub>8</sub>; **Table 2.1**). Thus, we conclude that mutation at residue 26 of CrtM directly alters the enzyme's specificity. Changing enzyme expression level or stability would not lead to increased C<sub>40</sub> performance and decreased C<sub>30</sub> performance of cultures expressing CrtM variants compared to those expressing wild-type CrtM (**Figure 2.6**). Variant M<sub>10</sub> possesses no mutation at amino acid position 26. Thus, it is apparent that mutation at this residue is not the only means by which CrtM can acquire CrtB-like activity. Of all 10 sequenced variants, M<sub>10</sub> is the only one with no substitution for phenylalanine at position 26 and is also the only one whose cultures did not have decreased C<sub>30</sub> pathway performance compared to CrtM cultures.

### Structural considerations: mapping mutations onto human squalene synthase

Most structurally characterized isoprenoid biosynthetic enzymes, including FPS, squalene synthase (SqS), and terpene cyclases, have the same “isoprenoid synthase fold,” consisting predominantly of  $\alpha$ -helices (22). In addition, secondary structure prediction (11) and sequence alignment (8) of CrtM and CrtB with their related enzymes also suggest that the enzymes have a common fold. Given this, and the lack of a crystal structure for a carotenoid synthase, we mapped the amino acid substitutions in our CrtM variants onto the crystal structure of human SqS (37).

SqSs catalyze the first committed step in cholesterol biosynthesis. As with carotene synthases, this is the head-to-head condensation of two identical prenyl

diphosphates (FPP for SqS). The condensation reaction catalyzed by SqS proceeds in two distinct steps (38). The first half-reaction generates the stable intermediate presqualene diphosphate, which forms upon abstraction of a diphosphate group from a prenyl donor, followed by 1-1' condensation of the donor and acceptor molecules. In the second half-reaction, the intermediate undergoes a complex rearrangement followed by a second removal of diphosphate and a final carbocation-quenching process (**Figure 2.7**). SqSs catalyze the additional reduction of the central double bond of 4,4'-diapophytoene (also called dehydrosqualene) by NADPH to form squalene, a reaction not performed by carotene synthases. Because the SqS and carotene synthase enzymes share clusters of conserved amino acids and catalyze essentially identical reactions, it is probable that they also have the same reaction mechanism. Indeed, when NADPH is in short supply, SqS produces 4,4'-diapophytoene, the natural product of CrtM (19, 52).

Sequence alignment of CrtM with related enzymes implies that F26 in CrtM corresponds to I58 in human SqS, which is located in helix B and points into the pocket that accommodates the second half-reaction. This residue is located four amino acids downstream of a flexible “flap” region in SqS that is believed to form a “lid” that shields intermediates in the reaction pocket from water (37). The amino acids constituting the flap are almost completely conserved among all known head-to-head isoprenoid synthase enzymes that catalyze 1-1' condensation.

It is noteworthy that a single mutation at F26 of CrtM is sufficient to permit this enzyme to synthesize C<sub>40</sub> carotenoids. Because this position is thought to lie in the site of the second half-reaction (rearrangement and quenching of a cyclopropylcarbinyl intermediate) (37), and because wild-type CrtM produces trace amounts of phytoene

(indicating that initially accepting two molecules of GGPP is not impossible), it is likely that wild-type CrtM is able to perform the first half-reaction of phytoene synthesis (condensation of two molecules of GGPP to form a presqualene diphosphate-like structure). We hypothesize that the F26 residue prevents the second half-reaction from going to completion by acting as a steric or electrostatic inhibitor of intermediate rearrangement. When this bulky phenylalanine residue is replaced with a smaller or more flexible amino acid such as serine or leucine, the second half-reaction is permitted to proceed and phytoene is produced.

Similar results for a variety of short-chain isoprenyl diphosphate synthases (IDSs) have been reported. In this class of enzymes, the size of the fifth amino acid upstream of the first aspartate-rich motif determines product length (29, 32, 33, 35, 36). Based on a very strong correlation between average product length and surface area of amino acids in this position (36), as well as the available crystal structure for avian FPS (47), it was hypothesized that this residue forms a steric barrier or wall that controls the size of the products (30). This model has been successfully applied to a variety of other enzymes in this family, including medium-chain IDSs (53). It is unknown why so many IDSs differing so greatly in sequence share a single key residue that determines product specificity.

### **Evolution of phytoene synthase (CrtB) in a C<sub>30</sub> pathway**

We constructed mutant libraries of *crtB* to search for variants with C<sub>30</sub> activity. Four mutagenic PCR libraries differing in MnCl<sub>2</sub> concentration were ligated into the *Xba*I-*Xho*I site of pUC-*crtB-crtN*, resulting in four pUC-*[crtB]-crtN* plasmid libraries. Upon transformation into XL1-Blue, pUC-*crtB-crtN*, containing wild-type *crtB*, gave no



discernible pigmentation, while the pUC-*crtM-crtN* cells produced had intense yellow pigmentation. Among the ~43,000 colonies expressing pUC-*[crtB]-crtN* variants screened, not a single one showed distinguishable yellow (or other) pigmentation. Thus, we found no CrtB mutants with improved C<sub>30</sub> activity. We also constructed five additional pUC-*[crtB]-crtN* libraries by using the Genemorph PCR mutagenesis kit (Stratagene), which enables the construction of randomly mutagenized gene libraries with a mutational spectrum different from that of those generated by mutagenic PCR with MnCl<sub>2</sub> (7). We screened an additional ~10,000 variants, but again found no variants of CrtB able to synthesize C<sub>30</sub> carotenoids at appreciable levels.

An explanation for the relative difficulty in acquiring C<sub>30</sub> function for CrtB may be that accepting a smaller-than-natural substrate is a more difficult task for this type of enzyme than accepting a larger-than-natural substrate. However, an evolutionary explanation may also be in order. The contexts in which the two enzymes evolved differ markedly. FPP is a precursor for many life-supporting compounds and is present in all organisms. Thus, C<sub>40</sub> enzymes such as CrtB have evolved in the presence of FPP throughout their history. It is not unreasonable to infer that CrtB has evolved under a nontrivial selection pressure to minimize consumption of FPP, for accepting FPP as a substrate and bypassing GGPP could be detrimental to the host organism's fitness. In stark contrast, C<sub>30</sub> synthases have evolved in an environment essentially devoid of GGPP. Consequently, no pressure to reject this substrate has been placed on these enzymes.

## CONCLUSIONS

We have demonstrated for the first time that the specificity of a carotenoid synthase is easily and profoundly altered by directed evolution. In our experiments, the carotene synthases CrtM and CrtB failed to complement one another in their respective foreign pathways. However, upon random mutagenesis of *crtM* followed by C<sub>40</sub>-specific color complementation screening, we isolated 116 mutants of the enzyme (~0.5% of the total screened) with significant C<sub>40</sub> activity. The *in vivo* C<sub>40</sub> pathway performance of the best CrtM variants is comparable to that of CrtB, the native C<sub>40</sub> synthase. That CrtM, a key biosynthetic enzyme that determines the size of the carotenoids in the downstream pathway, is capable of synthesizing C<sub>35</sub> carotenoid backbones and is one amino acid substitution from becoming a C<sub>40</sub> phytoene synthase is a finding of evolutionary and technological significance.

Firn and Jones have suggested that natural product biosynthetic pathways have evolved traits that enhance their ability to generate and retain chemical diversity in order to maximize their likelihood of discovering new biologically active molecules (13, 14, 20). The two major traits that Firn and Jones have identified in these pathways are the use of enzymes with broad substrate or product specificity and a high degree of pathway branching or bifurcation. Our work has revealed a special type of combinatorial pathway branching that exploits the precursor-fusion chemistry of carotenoid synthases. The native reaction catalyzed by CrtM is the condensation of two molecules of FPP to form a C<sub>30</sub> carotenoid backbone. Here we have shown that wild-type CrtM also possesses the ability to condense one molecule of FPP with one molecule of GGPP to form a C<sub>35</sub> carotenoid backbone. However, the enzyme is very poor at condensing two molecules of

GGPP to form the C<sub>40</sub> carotenoid backbone, phytoene. By broadening the specificity of CrtM through point mutagenesis, we have created variants that can also synthesize C<sub>40</sub> carotenoids. That these mutants can synthesize two non-native products as a result of the addition of only one new precursor (GGPP) to their substrate repertoires is a consequence of both their broadened specificity as well as the nature of the coupling reaction catalyzed by carotenoid synthases. If a (mutant) carotenoid synthase does not discriminate between  $n$  different prenyl diphosphate substrates, it will synthesize  $n(n+1)/2$  different carotenoid backbones by virtue of the combinatorics of substrate coupling. Therefore, carotenoid synthases, by virtue of their special chemistry, can act as key “diversity-multiplying” enzymes in carotenoid biosynthetic pathways if suitable mutants able to accept non-native precursors can be found. In the following chapter, we describe the continuation of our efforts to further expand carotenoid biosynthesis by creating additional backbones that can serve as new branch points for carotenoid pathway diversification.

## MATERIALS AND METHODS

### Materials

*Erwinia uredovora* (current approved name: *Pantoea ananatis*) C<sub>40</sub> carotenoid pathway genes *crtE* encoding GGPP (C<sub>20</sub>PP) synthase, *crtB* encoding phytoene synthase, and *crtI* encoding phytoene desaturase were obtained by genomic PCR as previously described (43). The *Escherichia coli* farnesyl diphosphate (FPP, C<sub>15</sub>PP) synthase gene *fps* was cloned from *E. coli* strain JM109. The C<sub>30</sub> pathway genes *crtM* (4,4'-diapophytoene synthase) and *crtN* (4,4'-diapophytoene desaturase) were cloned by PCR from *Staphylococcus aureus* genomic DNA (ATCC no. 35556D). We used *E. coli* XL1-Blue

supercompetent cells (Stratagene, La Jolla, CA) for cloning, screening, and carotenoid biosynthesis. AmpliTaq polymerase (Perkin-Elmer, Boston, MA) was employed for mutagenic PCR, while Vent polymerase (New England Biolabs, Beverly, MA) was used for cloning PCR. All chemicals and reagents used were of the highest available grade.

### **Plasmid construction**

Plasmid maps and sequences can be found in Appendix A. Plasmid pUC18m was constructed by removing the entire *lacZ* fragment and multi-cloning site from pUC18 and inserting the multi-restriction site sequence 5'-CATATG-GAATTC-TCTAGA-CTCGAG-GGGCCC-GGCGCC-3' (*NdeI-EcoRI-XbaI-XhoI-ApaI-EheI*). Each open reading frame following a Shine-Dalgarno ribosomal binding sequence (boldface) and a spacer (**AGGAGGATTACAAA**) was cloned into pUC18m (see Appendix A) to form artificial operons for acyclic C<sub>40</sub> carotenoids (pUC-*crtE-crtB-crtI*) or acyclic C<sub>30</sub> carotenoids (pUC-*fps-crtM-crtN* or pUC-*crtM-crtN*) (the genes in plasmids and operons are always listed in transcriptional order). To facilitate exchange between the two pathways, corresponding genes were flanked by the same restriction sites: isoprenyl diphosphate synthase genes (*fps* and *crtE*) were flanked by *EcoRI* and *XbaI* sites, carotene synthase genes (*crtM* and *crtB*) were flanked by *XbaI* and *XhoI* sites, and carotene desaturase genes (*crtN* and *crtI*) were flanked by *XhoI* and *ApaI* sites (**Figure 2.2a**).

### **Error-prone PCR mutagenesis and screening**

A pair of primers (5'-GCTGCCGTCAGTTAATCTAGAAGGAGG-3') and (5'-AGACGAATTGCCAGTGCCAGGCCACCG-3') flanking *crtM* were designed to amplify the 0.85-kb gene by PCR under mutagenic conditions: 5 U AmpliTaq (100 µl

total volume); 20 ng of template DNA (entire plasmid); 50 pmol of each primer; 0.2 mM dATP; 1.0 mM (each) dTTP, dGTP, and dCTP; and 5.5 mM MgCl<sub>2</sub>. Four different mutagenic libraries were made by using four different MnCl<sub>2</sub> concentrations: 0.2, 0.1, 0.05, and 0.02 mM. The temperature cycling scheme was 95 °C for 4 min followed by 30 cycles of 95 °C for 30 s, 40 °C for 45 s, and 72 °C for 2 min and by a final stage of 72 °C for 10 min. PCR yields for the 0.85-kb amplified fragment were 5 µg, corresponding to an amplification factor of ~1,000 or ~10 effective cycles. The PCR product from each library was purified with a Zymoclean gel purification kit (Zymo Research, Orange, CA), followed by digestion with *Xho*I and *Xba*I and *Dpn*I treatment to digest the template. The PCR products were ligated into the carotene synthase gene site of vector pUC-*crtE-crtM-crtI*, resulting in pUC-*crtE-[crtM]-crtI* libraries (square brackets indicate the randomly mutagenized gene). PCR mutagenesis of *crtB* on plasmid pUC-*crtB-crtN* was performed with primers 5'-CTTTACACTTTATGCTTCCGG-3' and 5'-TCCTGTGACACCTG CACCAATTACTGC-3' under the same conditions used for mutagenesis of *crtM*. The PCR products were purified, digested, and ligated as described above into the carotene synthase gene site of pUC-*crtB-crtN*, resulting in four pUC-*[crtB]-crtN* libraries.

The ligation mixtures were transformed into *E. coli* XL1-Blue supercompetent cells. Colonies were grown on Luria-Bertani (LB) plates containing carbenicillin (50 mg/l) as a selective marker at 37 °C for 12 h. Colonies were lifted onto white nitrocellulose membranes (Pall, Port Washington, NY), transferred onto LB+carbenicillin plates, and visually screened for color variants after an additional 12 to 24 h at room temperature. Selected colonies were picked and cultured overnight in 96-well plates, each well containing 0.5 ml of liquid LB medium supplemented with carbenicillin (50 mg/l).

## Pigment analysis

Among the strains we tested as expression hosts, XL1-Blue showed the best results in terms of stability and intensity of the color developed by colonies on agar plates. Although all of the genes assembled in each plasmid are grouped under a single *lac* operator/promoter, our expression system showed no response in terms of pigmentation levels to different IPTG (isopropyl- $\beta$ -D-thiogalactopyranoside) concentrations. Thus, leaky transcription from the *lac* promoter was sufficient for carotenoid production in *E. coli*. Based on this observation, all experiments described in this report were performed without IPTG induction.

To measure the relative amounts of carotenoids synthesized (see **Figure 2.6**), single colonies were inoculated into 3-ml precultures (LB medium containing 50 mg/l of carbenicillin) and shaken at 250 rpm and 37 °C overnight. Twenty microliters of each preculture were inoculated into 3 ml of Terrific broth (TB) medium (also containing 50 mg/l of carbenicillin) and shaken for 24 (C<sub>30</sub> carotenoid cultures) or 30 h (C<sub>40</sub> carotenoid cultures) at 250 rpm and 30 °C. The optical density at 600 nm (OD<sub>600</sub>) of each culture was measured immediately before harvesting. Then, 2 ml of each TB culture was centrifuged, the liquid was decanted, and the resulting cell pellet was extracted with 1 ml of acetone. The absorbance spectrum of each extract was measured with a SpectraMax Plus 384 microplate spectrophotometer (Molecular Devices, Sunnyvale, CA). Pigmentation levels in the culture extracts were determined from the height of absorption maxima ( $\lambda_{\text{max}}$ ): 470 nm for C<sub>30</sub> carotenoids and 475 nm for C<sub>40</sub> carotenoids.

For accurate determination of the carotenoids produced by the cultures, 500  $\mu$ l of LB preculture was inoculated into 50 ml of TB+carbenicillin (50 mg/l) and shaken in a

250-ml tissue culture flask (Becton Dickinson-Falcon, Bedford, MA) at 170 rpm and 30 °C for 24 to 30 h. Cultures expressing only CrtE plus a carotenoid synthase (CrtB, CrtM, or a mutant CrtM) were cultivated in 50 ml of TB+carbenicillin (50 mg/l) for 40 h at 160 rpm and 28 °C in 250-ml tissue culture flasks. The OD<sub>600</sub> of each culture was measured immediately before harvesting, and the dry cell mass was determined from this measurement by using a calibration curve generated for similar cultures. After centrifugation, the cell pellets were extracted with 10 ml of an acetone-methanol mixture (2:1 [vol/vol]). Pigments were concentrated, and the solvent was replaced with 20 ml of hexane. Then, an equal volume of aqueous NaCl (100 g/l) was added, and the mixture was shaken vigorously to remove oily lipids. The upper phase containing the carotenoids was dewatered with anhydrous MgSO<sub>4</sub> and concentrated in a rotary evaporator. The final volume of extract from each 50-ml culture was 1 ml. A 30- to 50-μl aliquot of extract was passed through a Spherisorb ODS2 column (4.6 × 250 mm, 5-μm particle size; Waters, Milford, MA) and eluted with an acetonitrile-isopropanol mixture (93:7 or 80:20 [vol/vol]) at a flow rate of 1 ml/min using an Alliance high-pressure liquid chromatography (HPLC) system (Waters) equipped with a photodiode array detector. Mass spectra were obtained with a series 1100 HPLC-mass spectrometer (Hewlett-Packard/Agilent, Palo Alto, CA) coupled with an atmospheric pressure chemical ionization interface.

The molar quantities of the carotenoid backbones shown in **Figure 2.5** were determined by comparing their HPLC chromatogram peak heights (at 286 nm) to a calibration curve generated using known amounts of a β,β-carotene standard (Sigma), and then multiplying by  $\epsilon_{\beta,\beta\text{-carotene (450 nm)}}/\epsilon_{\text{phytoene (286 nm)}}$ . The values of the molar

extinction coefficients ( $\epsilon$ ) used in the calculation were 138,900 and 49,800, respectively (6). The molar quantities of carotenoids were then normalized to the dry cell mass of each culture.



**Table 2.1.** Mutations found in sequenced CrtM variants

Mutant designation	Nonsynonymous mutations (amino acid change)	Synonymous mutations
M <sub>1</sub>	T76C (F26L) A364T (T122S)	A561G
M <sub>2</sub>	A58G (K20E) T77C (F26S)	A471T
M <sub>3</sub>	T76C (F26L) G127A (V43M)	A408G
M <sub>4</sub>	T76C(F26L) A446G (E149G)	T150C G489A A726G
M <sub>5</sub>	T76C (F26L) T800C (F267S)	
M <sub>6</sub>	A35G (H12R) T76C (F26L) A80G (D27G) A290G (K97R) A620G (H207R)	A688G
M <sub>7</sub>	T76C (F26L)	A186G A447G
M <sub>8</sub>	T78A (F26L)	A345G
M <sub>9</sub>	T77C (F26S) T119C (I40T)	T135C T141C
M <sub>10</sub>	A10G (M4V) A35G (H12R) T176C (F59S) A242G (Q81R) A539G (E180G)	A39G

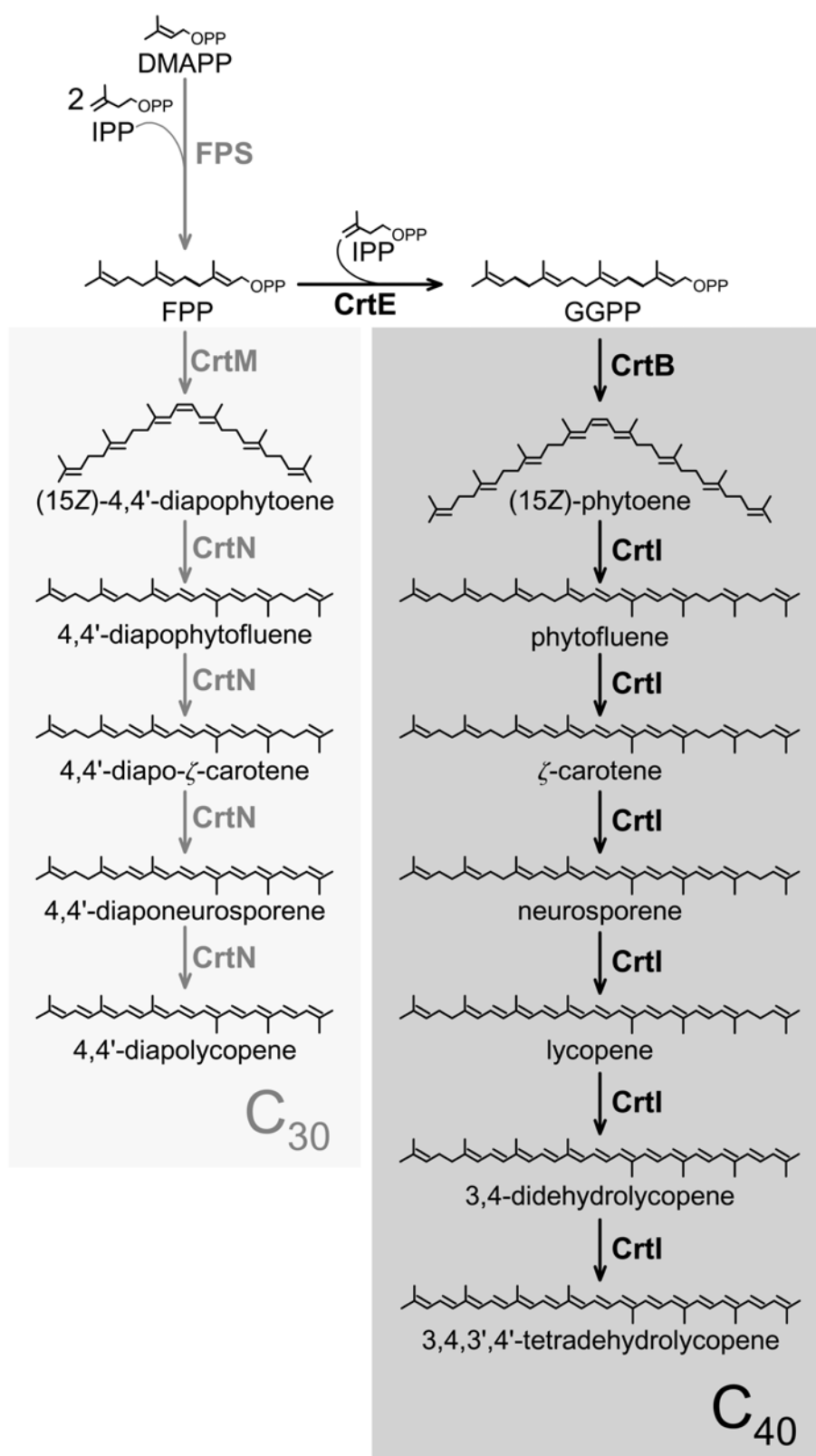
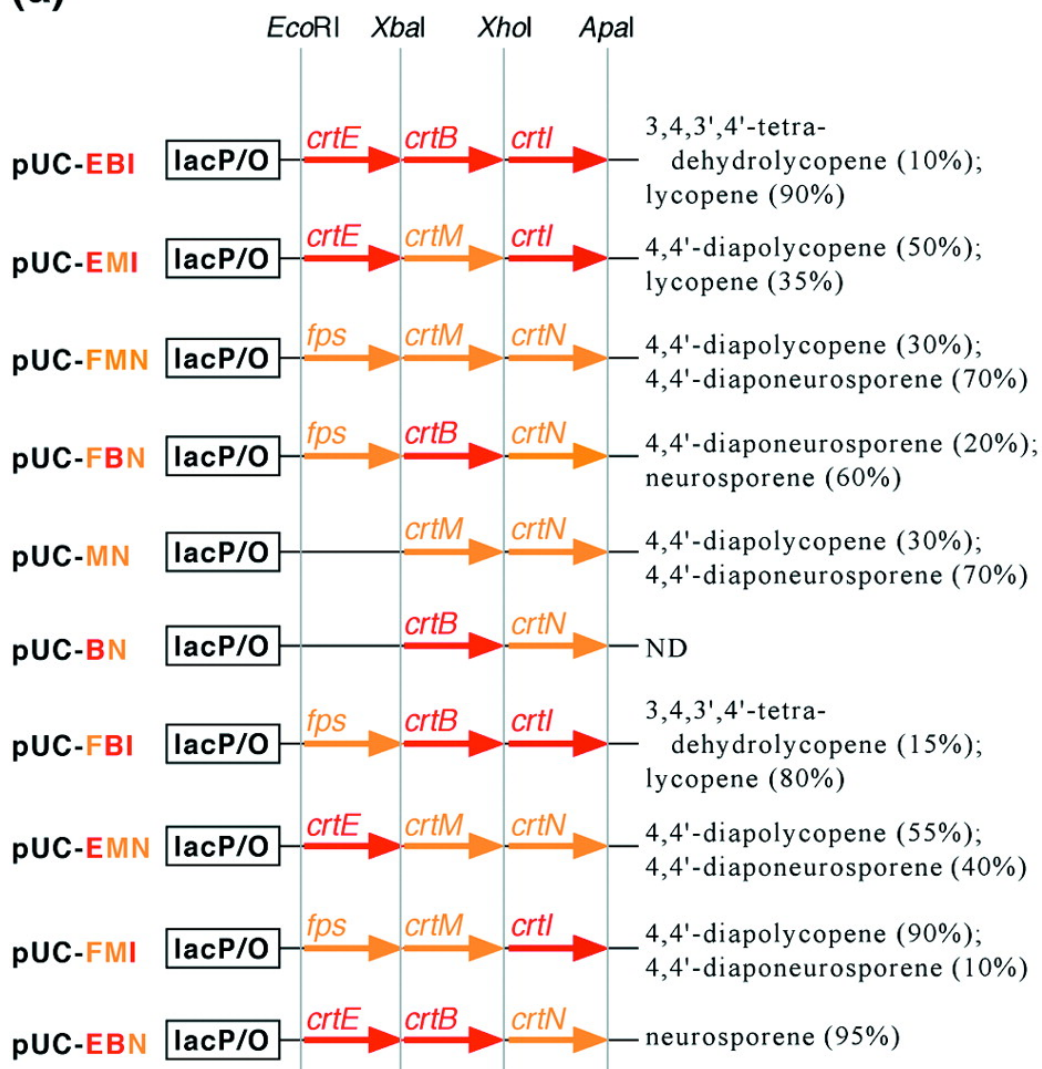


Figure 2.1

**Figure 2.1. Natural carotenoid biosynthetic pathways.** Carotenoid pathways are branches of the general isoprenoid pathway. In nature, two distinctive routes to carotenoid structures are known.  $C_{40}$  pathways, which start from the head-to-head condensation of two molecules of GGPP ( $C_{20}PP$ ), are found in a variety of plant and microbial species.  $C_{30}$  pathways, which begin with the condensation of two molecules of FPP ( $C_{15}PP$ ), have been identified only in a small number of bacterial species. Shown are the 15Z isomers of 4,4'-diapophytoene and phytoene, which are produced by CrtM and CrtB, respectively. Bacterial desaturases CrtN and CrtI catalyze *Z-E* isomerization of the central double bond in addition to desaturation of their carotenoid backbone substrates (15). The enzyme FPS is an FPP synthase; CrtE is a bacterial GGPP synthase; CrtM and CrtB are bacterial carotenoid synthases. DMAPP, dimethylallyl diphosphate; IPP, isopentenyl diphosphate.

(a)



(b)

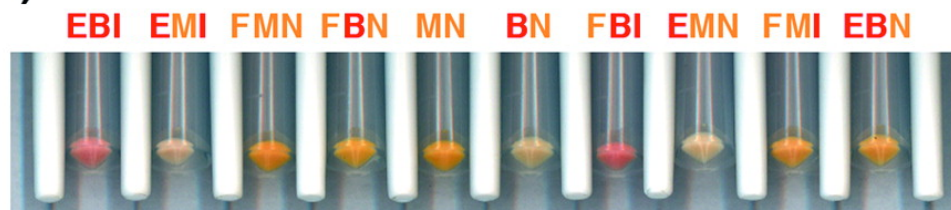


Figure 2.2

**Figure 2.2. C<sub>30</sub> and C<sub>40</sub> production systems used in this work.** (a) Plasmids used in this work. Under the control of the *lac* promoter and operator of a pUC18-derived plasmid, carotene synthase genes (*crtB* and *crtM*) were cloned into an *Xba*I-*Xho*I site, along with the isoprenyl diphosphate synthase genes (*crtE* and *fps*; *Eco*RI-*Xba*I site) and the carotene desaturase genes (*crtN* and *crtI*; *Xho*I-*Apa*I site). Listed on the right are the approximate mole percentages (as a fraction of total carotenoids) of the main carotenoids produced by *E. coli* XL1-Blue cells transformed with each plasmid. Only major species consisting of at least 10% of total carotenoids are shown. ND, none detected. (b) Cell pellets of XL1-Blue harboring various carotenogenic plasmids.

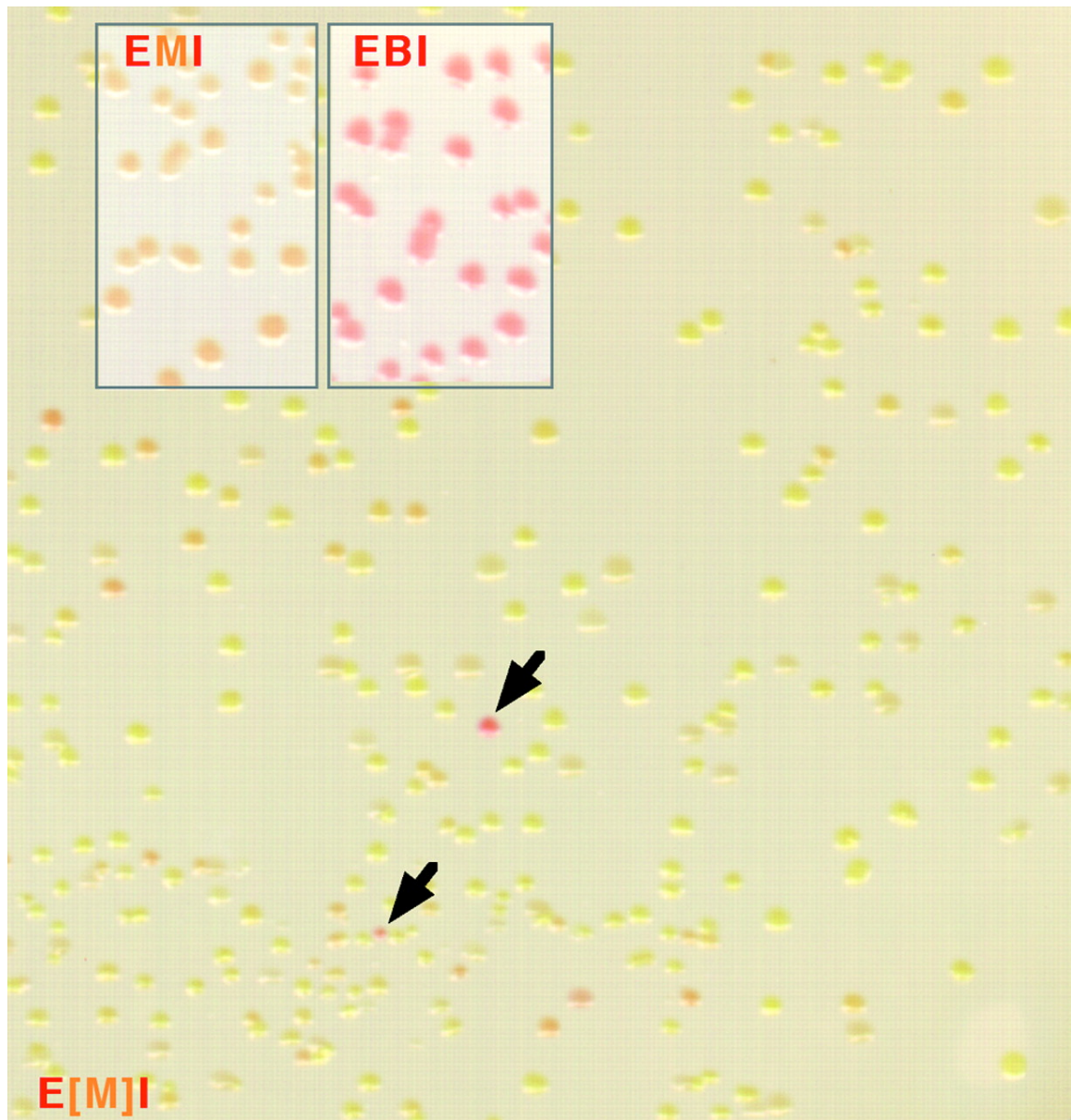


Figure 2.3

**Figure 2.3. Typical plate with *E. coli* XL1-Blue colonies expressing a mutagenic library of CrtM together with CrtI and CrtE.** XL1-Blue cells were transformed with pUC-*crtE*-[*crtM*]-*crtI* (E[M]I), where [*crtM*] represents a mutagenic library of *crtM*. Among a majority of pale colonies can be seen deep red-pink colonies (arrows) expressing CrtM variants that have acquired C<sub>40</sub> pathway functionality. EMI and EBI, XL1-Blue cells transformed with pUC-*crtE*-*crtM*-*crtI* and pUC-*crtE*-*crtB*-*crtI*, respectively.

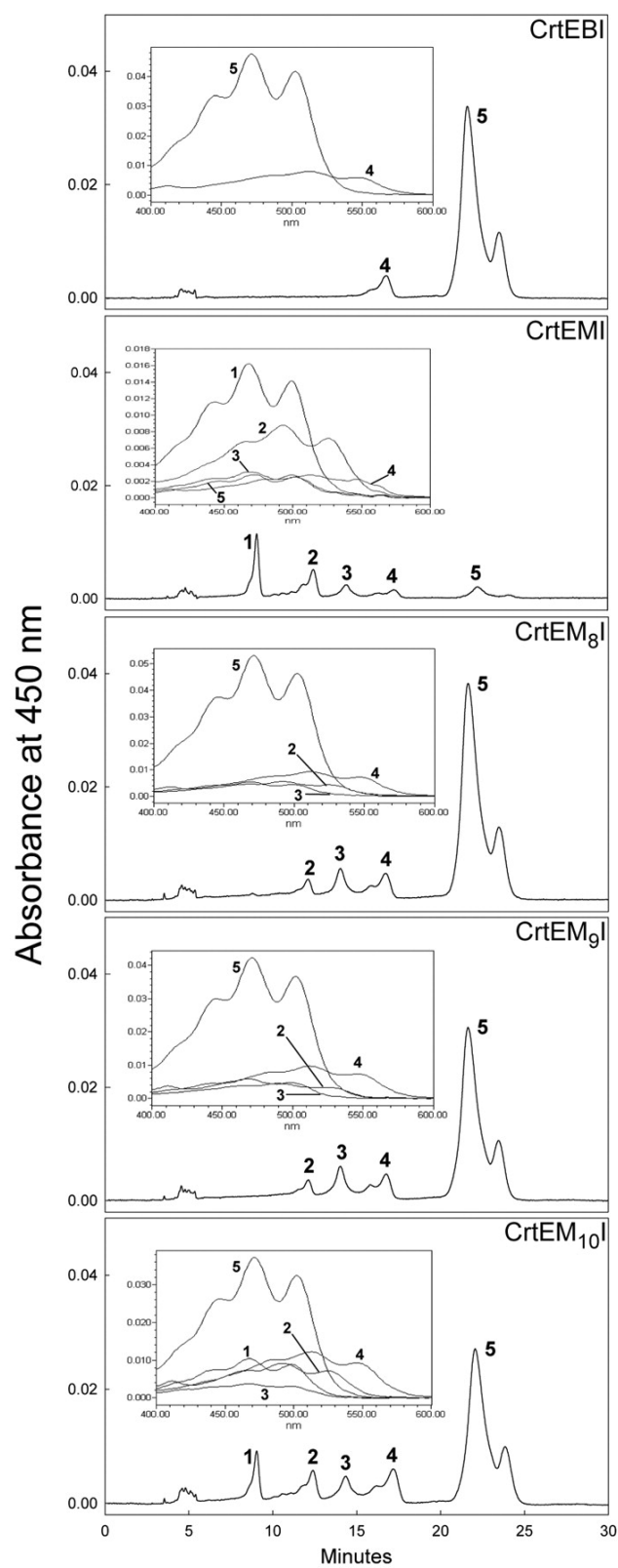
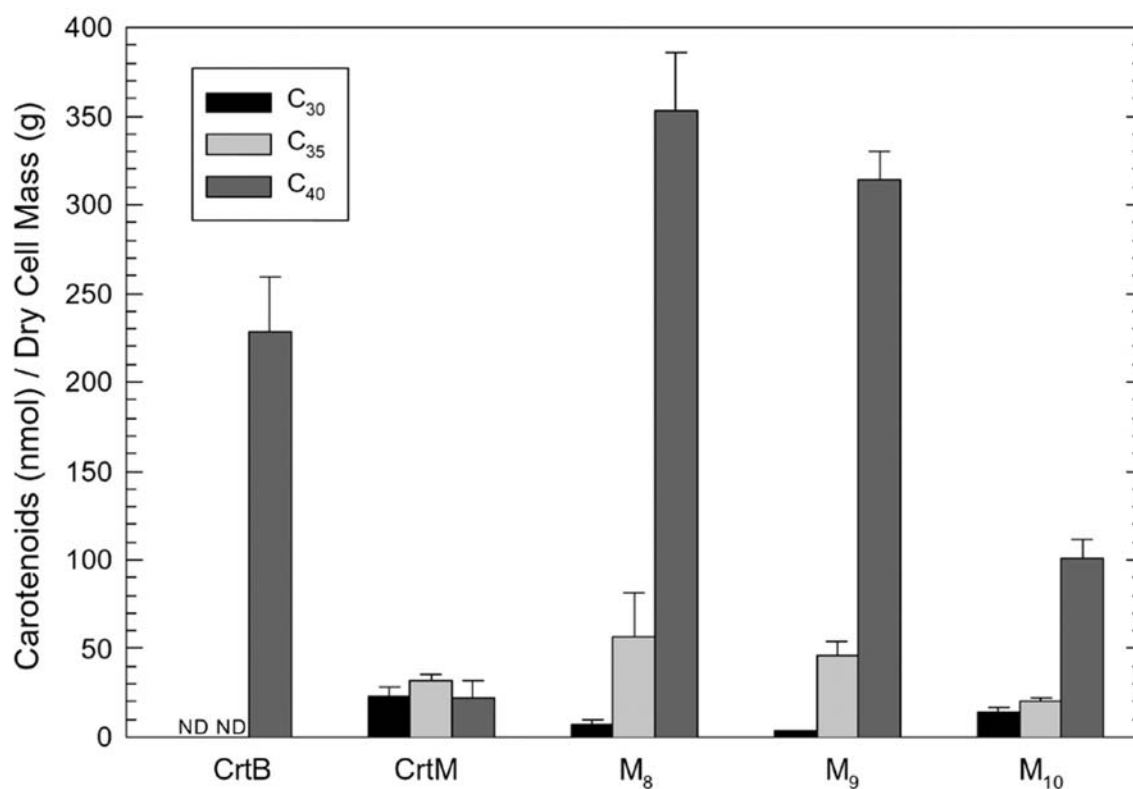


Figure 2.4



**Figure 2.4. HPLC-photodiode array analysis of carotenoid extracts of *E. coli* transformants carrying plasmids pUC-*crtE-crtB-crtI*, pUC-*crtE-crtM-crtI*, and pUC-*crtE-M<sub>8-10</sub>-crtI*.** The following carotenoids were identified: peak 1, 4,4'-diapolycopene ( $\lambda_{\text{max}}$  [nm]: 501, 470, 444,  $M^+$  at  $m/z = 400.4$ ); peak 2, 4-apo-3',4'-didehydrolycopene ( $\lambda_{\text{max}}$  [nm]: 527, 490, 465,  $M^+$  at  $m/z = 466.4$ ); peak 3, 4-apolycopene or 4-apo-3',4'-didehydro-7,8-dihydrolycopene ( $\lambda_{\text{max}}$  [nm]: 500, 470, 441,  $M^+$  at  $m/z = 468.4$ ); peak 4, 3,4,3',4'-tetrahydrolycopene ( $\lambda_{\text{max}}$  [nm]: 540, 510, 480,  $M^+$  at  $m/z = 532.4$ ); peak 5, lycopene ( $\lambda_{\text{max}}$  [nm]: 502, 470, 445,  $M^+$  at  $m/z = 536.5$ ). Double peaks indicate different geometrical isomers of the same compound. Insets, recorded absorption spectra of individual HPLC peaks.



**Figure 2.5. Direct product distribution of CrtM and its mutants in the presence of CrtE (GGPP supply).** Carotenoid extracts of XL1-Blue cells carrying plasmids pUC-*crtE-crtB*, pUC-*crtE-crtM*, and pUC-*crtE-M<sub>8-10</sub>* were analyzed by HPLC with a photodiode array detector. Peaks for 4,4'-diapophytoene (C<sub>30</sub>), 4-apophytoene (C<sub>35</sub>), and phytoene (C<sub>40</sub>) were monitored at 286 nm. Molar quantities of the various carotenoids were determined as described in Materials and Methods. Bar heights are normalized to dry cell mass, each represents the average of three independent cultures; error bars, standard deviations. ND, not detected.

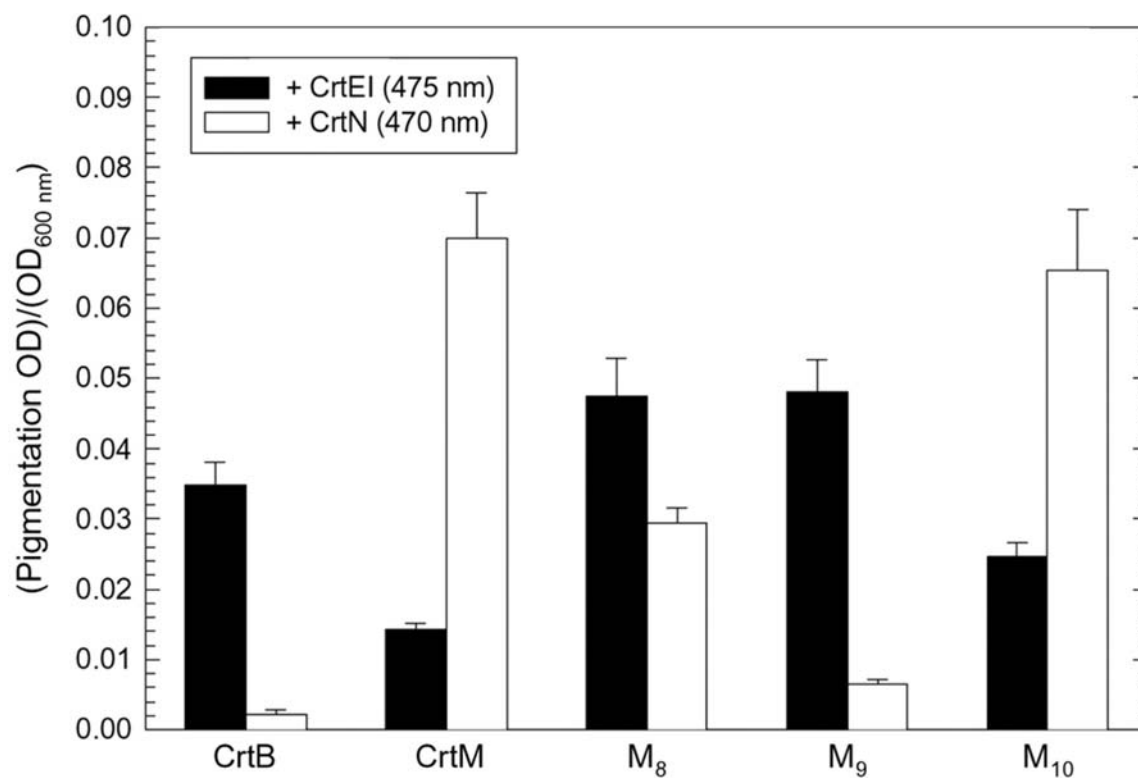


**Figure 2.6. Pigmentation produced by CrtM variants in C<sub>40</sub> and C<sub>30</sub> pathways.** XL1-Blue cells were transformed with either pUC-*crtE-M<sub>8-10</sub>-crtI* (C<sub>40</sub> pathway) or pUC-*M<sub>8-10</sub>-crtN* (C<sub>30</sub> pathway) and cultured in a test tube (3 ml of TB) as described in Materials and Methods. Pigmentation levels in the culture extracts were determined from the absorption peak height of  $\lambda_{\max}$  (470 nm for C<sub>30</sub> carotenoids, 475 nm for C<sub>40</sub> carotenoids) of each sample. Bar heights are normalized to OD<sub>600</sub> and represent the averages of at least three replicates; error bars, standard deviations.

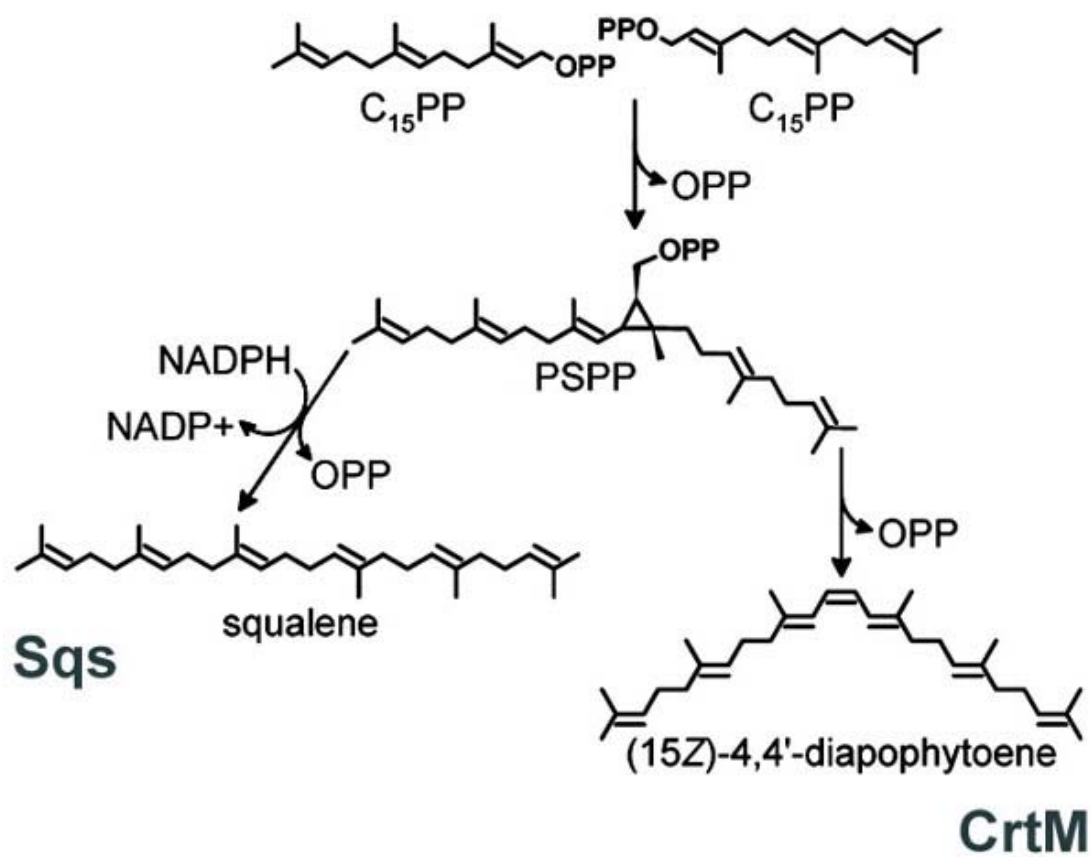


**Figure 2.7. Reaction schemes for Sqs and CrtM.** PSPP, presqualene diphosphate.

## REFERENCES

1. **Albrecht, M., S. Takaichi, N. Misawa, G. Schnurr, P. Boger, and G. Sandmann.** 1997. Synthesis of atypical cyclic and acyclic hydroxy carotenoids in *Escherichia coli* transformants. *J. Biotechnol.* **58**:177-185.
2. **Albrecht, M., S. Takaichi, S. Steiger, Z. Y. Wang, and G. Sandmann.** 2000. Novel hydroxycarotenoids with improved antioxidative properties produced by gene combination in *Escherichia coli*. *Nat. Biotechnol.* **18**:843-846.
3. **Armstrong, G. A., and J. E. Hearst.** 1996. Carotenoids 2: Genetics and molecular biology of carotenoid pigment biosynthesis. *Faseb J* **10**:228-37.
4. **Ben-Dor, A., A. Nahum, M. Danilenko, Y. Giat, W. Stahl, H. D. Martin, T. Emmerich, N. Noy, J. Levy, and Y. Sharoni.** 2001. Effects of acyclo-retinoic acid and lycopene on activation of the retinoic acid receptor and proliferation of mammary cancer cells. *Arch. Biochem. Biophys.* **391**:295-302.
5. **Britton, G.** 1998. Overview of carotenoid biosynthesis, p. 13-140. *In* G. Britton, S. Liaaen-Jensen, and H. Pfander (ed.). *Carotenoids vol. 3: Biosynthesis and Metabolism*. Birkhäuser Verlag, Basel.
6. **Britton, G.** 1995. UV/Visible Spectroscopy, p. 13-62. *In* G. Britton, S. Liaaen-Jensen, and H. Pfander (ed.). *Carotenoids, vol. 1B: Spectroscopy*. Birkhäuser Verlag, Basel.
7. **Cline, J., and H. Hogrefeo.** 1999. Randomize gene sequences with new PCR mutagenesis kit. *Stratagies* **13**:157-162.
8. **Corpet, F.** 1988. Multiple sequence alignment with hierarchical clustering. *Nucleic Acids Res.* **16**:10881-90.
9. **Crock, J., M. Wildung, and R. Croteau.** 1997. Isolation and bacterial expression of a sesquiterpene synthase cDNA clone from peppermint (*Mentha x piperita*, L.) that produces the aphid alarm pheromone (*E*)-beta-farnesene. *Proc. Natl. Acad. Sci. USA* **94**:12833-12838.
10. **Croteau, R., F. Karp, K. C. Wagschal, D. M. Satterwhite, D. C. Hyatt, and C. B. Skotland.** 1991. Biochemical characterization of a spearmint mutant that resembles peppermint in monoterpene content. *Plant Physiol.* **96**:744-752.
11. **Cuff, J. A., M. E. Clamp, A. S. Siddiqui, M. Finlay, and G. J. Barton.** 1998. JPred: a consensus secondary structure prediction server. *Bioinformatics* **14**:892-3.
12. **Facchini, P. J., and J. Chappell.** 1992. Gene family for an elicitor-induced sesquiterpene cyclase in tobacco. *Proc. Natl. Acad. Sci. USA* **89**:11088-11092.
13. **Firn, R. D., and C. G. Jones.** 2000. The evolution of secondary metabolism—a unifying model. *Mol. Microbiol.* **37**:989-994.
14. **Firn, R. D., and C. G. Jones.** 2003. Natural products—a simple model to explain chemical diversity. *Nat. Prod. Rep.* **20**:382-391.
15. **Fraser, P. D., N. Misawa, H. Linden, S. Yamano, K. Kobayashi, and G. Sandmann.** 1992. Expression in *Escherichia coli*, purification, and reactivation of the recombinant *Erwinia uredovora* phytoene desaturase. *J. Biol. Chem.* **267**:19891-19895.
16. **Garcia-Asua, G., H. P. Lang, C. N. Hunter, and R. J. Cogdell.** 1998. Carotenoid diversity: a modular role for the phytoene desaturase step. *Trends Plant Sci.* **3**:445-449.

17. **Hornero-Méndez, D., and G. Britton.** 2002. Involvement of NADPH in the cyclization reaction of carotenoid biosynthesis. *FEBS Lett.* **515**:133-136.
18. **Ishimi, Y., M. Ohmura, X. X. Wang, M. Yamaguchi, and S. Ikegami.** 1999. Inhibition by carotenoids and retinoic acid of osteoclast-like cell formation induced by bone-resorbing agents *in vitro*. *J. Clin. Biochem. Nutr.* **27**:113-122.
19. **Jarstfer, M. B., B. S. J. Blagg, D. H. Rogers, and C. D. Poulter.** 1996. Biosynthesis of squalene. Evidence for a tertiary cyclopropylcarbinyl cationic intermediate in the rearrangement of presqualene diphosphate to squalene. *J. Am. Chem. Soc.* **118**:13089-13090.
20. **Jones, C. G., and R. D. Firn.** 1991. On the evolution of plant secondary chemical diversity. *Philos. Trans. R. Soc. Lond. Ser. B-Biol. Sci.* **333**:273-280.
21. **Komori, M., R. Ghosh, S. Takaichi, Y. Hu, T. Mizoguchi, Y. Koyama, and M. Kuki.** 1998. A null lesion in the rhodopin 3,4-desaturase of *Rhodospirillum rubrum* unmasks a cryptic branch of the carotenoid biosynthetic pathway. *Biochemistry* **37**:8987-8994.
22. **Lesburg, C. A., J. M. Caruthers, C. M. Paschall, and D. W. Christianson.** 1998. Managing and manipulating carbocations in biology: terpenoid cyclase structure and mechanism. *Curr. Opin. Struct. Biol.* **8**:695-703.
23. **Linden, H., N. Misawa, D. Chamovitz, I. Pecker, J. Hirschberg, and G. Sandmann.** 1991. Functional complementation in *Escherichia coli* of different phytoene desaturase genes and analysis of accumulated carotenes. *Z. Naturforsch. (C)* **46**:1045-1051.
24. **LinGoerke, J. L., D. J. Robbins, and J. D. Burczak.** 1997. PCR-based random mutagenesis using manganese and reduced dNTP concentration. *Biotechniques* **23**:409-412.
25. **Matsuoka, S., H. Sagami, A. Kurisaki, and K. Ogura** 1991. Variable product specificity of microsomal dehydrodolichyl diphosphate synthase from rat liver. *J. Biol. Chem.* **266**:3464-3468.
26. **Mayne, S. T.** 1996. Beta-carotene, carotenoids, and disease prevention in humans. *Faseb J.* **10**:690-701.
27. **Nagaki, M., S. Sato, Y. Maki, T. Nishino, and T. Koyama.** 2000. Artificial substrates for undecaprenyl diphosphate synthase from *Micrococcus luteus* B-P 26. *J. Mol. Catal. B-Enzym.* **9**:33-38.
28. **Nagaki, M., A. Takaya, Y. Maki, J. Ishibashi, Y. Kato, T. Nishino, and T. Koyama.** 2000. One-pot syntheses of the sex pheromone homologs of a codling moth, *Laspeyresia promonella* L. *J. Mol. Catal. B-Enzym.* **10**:517-522.
29. **Narita, K., S. Ohnuma, and T. Nishino.** 1999. Protein design of geranyl diphosphate synthase. Structural features that define the product specificities of prenyltransferases. *J Biochem (Tokyo)* **126**:566-71.
30. **Ogura, K., and T. Koyama.** 1998. Enzymatic aspects of isoprenoid chain elongation. *Chem. Rev.* **98**:1263-1276.
31. **Ohnuma, S., H. Hemmi, T. Koyama, K. Ogura, and T. Nishino.** 1998. Recognition of allylic substrates in *Sulfolobus acidocaldarius* geranylgeranyl diphosphate synthase: Analysis using mutated enzymes and artificial allylic substrates. *J. Biochem. (Tokyo)* **123**:1036-1040.

32. **Ohnuma, S., K. Hirooka, H. Hemmi, C. Ishida, C. Ohto, and T. Nishino.** 1996. Conversion of product specificity of archaeobacterial geranylgeranyl-diphosphate synthase—identification of essential amino acid residues for chain length determination of prenyltransferase reaction. *J. Biol. Chem.* **271**:18831-18837.
33. **Ohnuma, S., K. Hirooka, C. Ohto, and T. Nishino.** 1997. Conversion from archaeal geranylgeranyl diphosphate synthase to farnesyl diphosphate synthase—Two amino acids before the first aspartate-rich motif solely determine eukaryotic farnesyl diphosphate synthase activity. *J. Biol. Chem.* **272**:5192-5198.
34. **Ohnuma, S., T. Koyama, and K. Ogura** 1993. Alternation of the product specificities of prenyltransferases by metal ions. *Biochem. Biophys. Res. Commun.* **192**:407-412.
35. **Ohnuma, S., T. Nakazawa, H. Hemmi, A. M. Hallberg, T. Koyama, K. Ogura, and T. Nishino.** 1996. Conversion from farnesyl diphosphate synthase to geranylgeranyl diphosphate synthase by random chemical mutagenesis. *J. Biol. Chem.* **271**:10087-10095.
36. **Ohnuma, S., K. Narita, T. Nakazawa, C. Ishida, Y. Takeuchi, C. Ohto, and T. Nishino.** 1996. A role of the amino acid residue located on the fifth position before the first aspartate-rich motif of farnesyl diphosphate synthase on determination of the final product. *J. Biol. Chem.* **271**:30748-30754.
37. **Pandit, J., D. E. Danley, G. K. Schulte, S. Mazzalupo, T. A. Pauly, C. M. Hayward, E. S. Hamanaka, J. F. Thompson, and H. J. Harwood.** 2000. Crystal structure of human squalene synthase—A key enzyme in cholesterol biosynthesis. *J. Biol. Chem.* **275**:30610-30617.
38. **Poulter, C. D., T. L. Capson, M. D. Thompson, and R. S. Bard.** 1989. Squalene synthetase—inhibition by ammonium analogs of carbocationic intermediates in the conversion of presqualene diphosphate to squalene. *J. Am. Chem. Soc.* **111**:3734-3739.
39. **Raisig, A., and G. Sandmann.** 2001. Functional properties of diapophytoene and related desaturases of C<sub>30</sub> and C<sub>40</sub> carotenoid biosynthetic pathways. *Biochim. Biophys. Acta Mol. Cell Biol. Lipids* **1533**:164-170.
40. **Redmond, T. M., S. Gentleman, T. Duncan, S. Yu, B. Wiggert, E. Gantt, and F. X. Cunningham.** 2001. Identification, expression, and substrate specificity of a mammalian beta-carotene 15,15'-dioxygenase. *J. Biol. Chem.* **276**:6560-6565.
41. **Reed, B. C., and H. C. Rilling.** 1976. Substrate binding of avian liver prenyltransferase. *Biochemistry* **15**:3739-45.
42. **Sacchettini, J. C., and C. D. Poulter.** 1997. Creating isoprenoid diversity. *Science* **277**:1788-1789.
43. **Schmidt-Dannert, C., D. Umeno, and F. H. Arnold.** 2000. Molecular breeding of carotenoid biosynthetic pathways. *Nat Biotechnol* **18**:750-3.
44. **Schnurr, G., N. Misawa, and G. Sandmann.** 1996. Expression, purification and properties of lycopene cyclase from *Erwinia uredovora*. *Biochem. J.* **315**:869-74.
45. **Steele, C. L., J. Crock, J. Bohlmann, and R. Croteau.** 1998. Sesquiterpene synthases from grand fir (*Abies grandis*)—comparison of constitutive and wound-induced activities, and cDNA isolation, characterization and bacterial expression of delta-selinene synthase and gamma-humulene synthase. *J. Biol. Chem.* **273**:2078-2089.

46. **Takaichi, S., K. Inoue, M. Akaike, M. Kobayashi, H. Ohoka, and M. T. Madigan.** 1997. The major carotenoid in all known species of heliobacteria is the C<sub>30</sub> carotenoid 4,4'-diaponeurosporene, not neurosporene. *Arch. Microbiol.* **168**:277-281.
47. **Tarshis, L. C., M. J. Yan, C. D. Poulter, and J. C. Sacchettini.** 1994. Crystal structure of recombinant farnesyl diphosphate synthase at 2.6-angstrom resolution. *Biochemistry* **33**:10871-10877.
48. **Taylor, R. F.** 1984. Bacterial triterpenoids. *Microbiol. Rev.* **48**:181-198.
49. **Taylor, R. F., and B. H. Davies.** 1974. Triterpenoid carotenoids of *Streptococcus faecium* UNH 564P. *Biochem. J.* **139**:751-760.
50. **Wang, C. W., and J. C. Liao.** 2001. Alteration of product specificity of *Rhodobacter sphaeroides* phytoene desaturase by directed evolution. *J. Biol. Chem.* **276**:41161-41164.
51. **Wieland, B., C. Feil, E. Gloriamercker, G. Thumm, M. Lechner, J. M. Bravo, K. Poralla, and F. Gotz.** 1994. Genetic and biochemical analyses of the biosynthesis of the yellow carotenoid 4,4'-diaponeurosporene of *Staphylococcus aureus*. *J. Bacteriol.* **176**:7719-7726.
52. **Zhang, D. L., and C. D. Poulter.** 1995. Biosynthesis of non-head-to-tail isoprenoids—Synthesis of 1'-1-structures and 1'-3-structures by recombinant yeast squalene synthase. *J. Am. Chem. Soc.* **117**:1641-1642.
53. **Zhang, Y. W., X. Y. Li, and T. Koyama.** 2000. Chain length determination of prenyltransferases: both heteromeric subunits of medium-chain (*E*)-prenyl diphosphate synthase are involved in the product chain length determination. *Biochemistry* **39**:12717-12722.
54. **Zhao, H., J. C. Moore, A. Volkov, and F. H. Arnold.** 1999. Methods for optimizing industrial enzymes by directed evolution, p. 597-604. *In* A. L. Demain and J. E. Davies (ed.). *Methods of Industrial Microbiology and Biotechnology*. 2nd ed, ASM Press, Washington DC.